

An effective method to calculate the electron impact excitation cross sections of helium from ground state to a final channel in the whole energy region

Rui Sun(孙瑞), De-Ling Zeng(曾德灵), Rui Jin(金锐), Xiao-Ying Han(韩小英), Xiang Gao(高翔), and Jia-Ming Li(李家明)

Citation: Chin. Phys. B, 2023, 32 (**11**): 113401. DOI: 10.1088/1674-1056/acf11f
Journal homepage: http://cpb.iphy.ac.cn; http://iopscience.iop.org/cpb

What follows is a list of articles you may be interested in

Fragmentation dynamics of electron-impact double ionization of helium

Shiwei Liu(刘士炜), Difa Ye(叶地发), and Jie Liu(刘杰)
Chin. Phys. B, 2023, 32 (**6**): 063402. DOI: 10.1088/1674-1056/acbe33

Electron excitation processes in low energy collisions of hydrogen-helium atoms

Kun Wang(王堃), Chuan Dong(董川), Yi-Zhi Qu(屈一至), Ling Liu(刘玲), Yong Wu(吴勇),Xu-Hai Hong(洪许海), and Robert J. Buenker
Chin. Phys. B, 2022, 31 (**12**): 123401. DOI: 10.1088/1674-1056/aca14c

Debye-screening effect on electron-impact excitation of helium-like Al^{11+} and Fe^{24+} ions

Yu-Long Ma(马玉龙), Ling Liu(刘玲), Lu-You Xie(颉录有), Yong Wu(吴勇), Deng-Hong Zhang(张登红), Chen-Zhong Dong(董晨钟), Yi-Zhi Qu(屈一至), and Jian-Guo Wang(王建国)
Chin. Phys. B, 2022, 31 (**4**): 043401. DOI: 10.1088/1674-1056/ac2e65

Resonances for positron-helium and positron-lithium systems in kappa-distribution plasma

Zi-Shi Jiang(姜子实), Ya-Chen Gao(高亚臣), Sabyasachi Kar, Kurunathan Ratnavelu
Chin. Phys. B, 2018, 27 (**12**): 123402. DOI: 10.1088/1674-1056/27/12/123402

Analysis of the fractal intrinsic quality in the ionization of Rydberg helium and lithium atoms

Yanhui Zhang(张延惠), Xiulan Xu(徐秀兰), Lisha Kang(康丽莎), Xiangji Cai(蔡祥吉), Xu Tang(唐旭)
Chin. Phys. B, 2018, 27 (**5**): 053401. DOI: 10.1088/1674-1056/27/5/053401

DATA PAPER

An effective method to calculate the electron impact excitation cross sections of helium from ground state to a final channel in the whole energy region

Rui Sun(孙瑞)[1,2,3,†], De-Ling Zeng(曾德灵)[4,†], Rui Jin(金锐)[5], Xiao-Ying Han(韩小英)[3], Xiang Gao(高翔)[3,‡], and Jia-Ming Li(李家明)[1,6]

[1] *Key Laboratory for Laser Plasmas, Ministry of Education, School of Physics and Astronomy, Shanghai Jiao Tong University, Shanghai* 200240, *China*
[2] *Collaborative Innovation Center of IFSA, Shanghai Jiao Tong University, Shanghai* 200240, *China*
[3] *Institute of Applied Physics and Computational Mathematics, Beijing* 100088, *China*
[4] *Institute of Electron & Electronic Measurement Technology, Shanghai Institute of Measurement and Testing Technology, Shanghai* 201203, *China*
[5] *Max-Planck-Institut für Kernphysik Saupfercheckweg* 169117, *Heidelberg, German*
[6] *Department of Physics and Center for Atomic and Molecular Nanosciences, Tsinghua University, Beijing* 100084, *China*

(Received 12 June 2023; revised manuscript received 2 August 2023; accepted manuscript online 17 August 2023)

The electron impact excitation (EIE) cross sections of an atom/ion in the whole energy region are needed in many research fields, such as astrophysics studies, inertial confinement fusion researches and so on. In the present work, an effective method to calculate the EIE cross sections of an atom/ion in the whole energy region is presented. We use the EIE cross sections of helium as an illustration example. The optical forbidden $1\,^1\mathrm{S}$–$n\,^1\mathrm{S}$ ($n = 2$–4) and optical allowed $1\,^1\mathrm{S}$–$n\,^1\mathrm{P}$ ($n = 2$–4) excitation cross sections are calculated in the whole energy region using the scheme that combines the partial wave R-matrix method and the first Born approximation. The calculated cross sections are in good agreement with the available experimental measurements. Based on these accurate cross sections of our calculation, we find that the ratios between the accurate cross sections and Born cross sections are nearly the same for different excitation final states in the same channel. According to this interesting property, a universal correction function is proposed and given to calculate the accurate EIE cross sections with the same computational efforts of the widely used Born cross sections, which should be very useful in the related application fields. The datasets presented in this paper are openly available at https://www.doi.org/10.57760/sciencedb.j00113.00142.

Keywords: the electron impact excitation cross sections, correction function, helium, the partial wave R-matrix plus the first Born approximation method

PACS: 34.80.Dp, 31.15.A–, 31.15.vj **DOI:** 10.1088/1674-1056/acf11f

1. Introduction

Electron impact excitation (EIE) cross sections of an atom/ion in a wide energy range (i.e., from thresholds to above 10× thresholds) are indispensable physical parameters in astrophysics studies, inertial confinement fusion researches and so on. For example, helium is an abundant element in the universe. Accurate and reliable helium abundances are needed to calculate the primordial helium abundance by unit mass Y_p, which is important for the study of cosmology and the chemical evolution of galaxies.[1–3] To obtain the helium abundance in astrophysics studies, one needs to estimate the contribution to the He I line intensities due to the collisional excitation, where the accurate EIE cross sections are essential.[4,5] Clegg showed for a sample of planetary nebulae (PNs) that the collision-to-recombination (C/R) correction (strongly dependent on the EIE cross sections) lowered the calculated He abundances by an average value of 10%.[4]

Many experimental studies[6–8] and theoretical calculations[9–14] have been carried out to investigate the EIE cross sections of He in the last decades. However, most of the calculations focus on a specific energy region (either on low or high energy region). The studies of EIE cross sections in the whole energy region are very limited. Fursa and Bray applied the convergent close-coupling (CCC) method to calculate e + He scattering cross sections excited from the ground state in the incident energy range from 1.5 eV to 500 eV,[13] where the overall agreement with the experimental data is good, but without detailed resonance structures. It will also take large computational efforts for the CCC method to exhibit the cross sections in the whole energy region because it can only concentrate on a single energy at a time. It is known that, in the low incident energy region, the EIE cross sections with complex resonant structures near thresholds can be accurately calculated by the partial wave expansion method such as R-matrix method.[15–17] In the high incident energy region, the first Born approximation (FBA) is applicable and the EIE

†These authors contributed equally to this paper.
‡Corresponding author. E-mail: gao_xiang@iapcm.ac.cn

© 2023 Chinese Physical Society and IOP Publishing Ltd

cross sections can be obtained from the generalized oscillator strengths (GOS).[18–22] Note that the quality of the target state wavefunctions is crucial for both partial wave expansion and GOS calculations.[14,18] Therefore, to calculate the EIE cross sections in the whole energy region efficiently, different methods should be used for different energy regions.[21] We have demonstrated for the e + He collision processes that the EIE cross sections of partial wave R-matrix method calculations can interface with the Born cross sections.[21]

In the present work, we propose an effective method to conveniently calculate the EIE cross sections with enough accuracy in the whole energy region. The e + He collision processes are used as an illustration example to show the validity and efficiency of our method. To facilitate the discussion, we will focus on the spin-allowed transitions. Because the spin-forbidden transitions are caused by the exchange interaction, then the FBA calculation should involve the matrix elements between the bound target electron and the scattering plane wave,[23,24] which makes these transitions usually less important in the high energy region[22] and would induce other complexity such as the non-orthogonality problem.[25] Considering the computational efforts are very large to use the R-matrix method alone below the FBA calculation region, we extend the calculation scheme presented in Ref. [21] by using the distorted wave (DW) approximation[26,27] calculations in the intermediate energy region between the R-matrix calculation region and FBA calculation region. The application of the DW method makes the interface of the EIE cross sections between different energy regions more effective. The accurate EIE cross sections of optical forbidden $1\,^1\mathrm{S}$–$n\,^1\mathrm{S}$ ($n = 2$–4) and optical allowed $1\,^1\mathrm{S}$–$n\,^1\mathrm{P}$ ($n = 2$–4) transitions are calculated using our extended scheme, which are in good agreement with the available experimental measurements.[28–32] Based on these accurate cross sections, we find that the ratios between these cross sections and the Born cross sections are nearly the same for different excitation final states belonging to the same channel. Then a universal correction function (CF) is proposed[16] and given to calculate the accurate EIE cross sections in the whole energy region with the same computational efforts of the Born cross sections, which may satisfy the needs in the related application fields.

2. Theory

To obtain the EIE cross sections of an atom/ion in the whole energy region from low to high, one should use different methods in the corresponding energy region. At low energy region, the interactions between the colliding electron and the target electrons involve electron exchange and correlation interactions, which is a many-body problem. The partial wave expansion method such as R-matrix method[15–17,34] is good to deal with these problems. At high incident energy region, the first Born approximation (FBA) is applicable[22,35–40] and various cross sections can be readily calculated as a whole instead of partial wave expansion. At the intermediate energy region, the distorted wave calculation can be applied, making the interface of EIE cross sections from low to high more effective. These three methods are all well-established methods detailed in many references.[22,27,34,35,41–43] Only some useful formulas are reviewed here for the sake of our following discussions.

The scattering matrices $\boldsymbol{S}$ is related to the transition matrices $\boldsymbol{T}$ by

$$\boldsymbol{T} = \boldsymbol{S} - 1. \tag{1}$$

The total cross sections from the R-matrix method for excitation from target state i to target state j in LS coupling is given from the $\boldsymbol{T}$ matrices by[34]

$$\begin{aligned}\sigma_{ij}^{(R\text{-matrix})} &= \frac{\pi}{k_i^2[\widetilde{L}][\widetilde{S}]}\sum_{LS\pi}^{N}\frac{[L][S]}{2}\sum_{l_i l_j}\left|T_{ij}^{LS}\right|^2 \\ &= \sum_{LS\pi}^{N}\sigma_L^{(R\text{-mat})LS\pi}.\end{aligned} \tag{2}$$

Here N represents the number of all relevant partial waves, L, S and π are the total orbital angular momenta, spin angular momentum and parity, respectively. $[L] = (2L+1)$, $[S] = (2S+1)$, l and k^2 are the channel angular momenta and energies. σ_L is the corresponding partial cross section.

In high energy region, the FBA is valid and the incident and scattered electrons can be treated as plane waves. Within the FBA, the generalized oscillator strength (GOS) is defined as[22,35–39]

$$F_{ij}(\Delta E, K) = \frac{2\Delta E}{K^2}\left|\left\langle \Phi_j(\widetilde{L'}\widetilde{S'}\widetilde{\pi'})\left|\sum_{\alpha=1}^{N}\mathrm{e}^{\mathrm{i}K\cdot r_\alpha}\right|\Phi_i(\widetilde{LS}\widetilde{\pi})\right\rangle\right|^2, \tag{3}$$

where ΔE is the energy transfer (i.e., excitation energy). K is the momentum transfer related to the scattering angle. Φ_i and Φ_j are the wavefunctions of the target atom for the initial and final states, respectively. r_α represents the coordinate of the αth target electron, the coordinate origin is the center of mass of the target.

The differential cross section (DCS) is proportional to the GOS as

$$\frac{\mathrm{d}\sigma_{ij}^{(\mathrm{FBA})}(\widehat{k'})}{\mathrm{d}\Omega} = \frac{2}{\Delta E}\frac{k'}{k}\frac{F_{ij}(\Delta E, K)}{K^2}. \tag{4}$$

The k and k' are the scattered electron momentums of the initial and final states, respectively. After performing the summation of the final state and the average of the initial state, we can obtain the FBA total cross section as

$$\sigma_{ij,\mathrm{total}}^{(\mathrm{FBA})} = \int\frac{\mathrm{d}\sigma_{i\to j}^{(\mathrm{FBA})}}{\mathrm{d}\Omega}2\pi\sin\theta\,\mathrm{d}\theta$$

$$= \int \frac{2}{\Delta E}\frac{k'}{k}\frac{F_{ij}(\Delta E,K)}{K^2}\frac{\pi \mathrm{d}(K^2)}{kk'}$$
$$= \int \frac{2\pi F_{ij}(\Delta E,K)}{\Delta E k^2}\mathrm{d}(\ln K^2). \quad (5)$$

When the incident energy is high enough, the FBA total cross sections become accurate total cross sections, i.e., $\sigma_{\text{total}}^{(\text{FBA})} \to \sigma_{\text{total}}^{(\text{accurate})}$. Also, the partial wave cross section (PWCS) within FBA is

$$\sigma_{ij,L}^{(\text{FBA})} = \frac{\pi}{k_i^2\left[\widetilde{L}\right]\left[\widetilde{S}\right]}\frac{[L][S]}{2}\sum_{l_i l_j}\left|T_{ij}^{((\text{FBA}))LS\pi}\right|^2$$
$$= \frac{\pi}{k_i^2\left[\widetilde{L}\right]\left[\widetilde{S}\right]}\frac{[L][S]}{2}\sum_{l_i l_j}\left|\left\langle \phi'_{l_j}, \Phi_j(\widetilde{L'S'}\widetilde{\pi'})\left|\sum_{\alpha=1}^{N}\frac{1}{|r-r_\alpha|}\right|\phi_{l_i}, \Phi_i(\widetilde{LS}\widetilde{\pi})\right\rangle\right|^2. \quad (6)$$

The ϕ_{l_i} and ϕ'_{l_j} are partial wave wavefunctions of continuum electron, which are the regular spherical Bessel functions here.

In our previous work,[21] we have presented a scheme for dealing with the EIE cross sections of atoms at low to high incident energies in a consistent way. We calculated the exact PWCS ($\sigma_L^{(R\text{-matrix})}$) and the FBA PWCS ($\sigma_L^{(\text{FBA})}$) in the energy region from low to high. Our calculation results show that when incident energy is high enough, the two kinds of PWCS decrease with increasing angular momentum L and increasing incident energy. The comparisons between the two kinds of PWCS manifest that the exact and FBA PWCSs merge together gradually with increasing L. The two features give some hint that the difference between the exact and FBA total cross sections mainly originates from the lowest PWCSs. Thus the approach of combining the partial wave method and the FBA is presented, i.e., replacing a few $\sigma_L^{(\text{FBA})}$ ($L < L_{\text{cut}}$) of the FBA total cross sections by the corresponding $\sigma_L^{(R\text{-matrix})}$. More specifically, we define the difference between $\sigma_L^{(R\text{-matrix})}$ and $\sigma_L^{(\text{FBA})}$ as $\sigma_L^{(\text{C})}$,

$$\sigma_L^{(\text{C})} = \sigma_L^{(R\text{-matrix})} - \sigma_L^{(\text{FBA})}. \quad (7)$$

If $\sigma_L^{(\text{C})}$ decreases quickly with increasing angular momentum L, the convergent total cross sections can be obtained by the FBA total cross sections plus limited $\sigma_L^{(\text{C})}$, i.e.,

$$\sigma_{\text{total}}^{(\text{accurate})} = \sigma_{\text{total}}^{(\text{FBA})} + \sum_{L=0}^{L_{\text{cut}}}\sigma_L^{(\text{C})}$$
$$= \sigma_{\text{total}}^{(\text{FBA})} + \sum_{L=0}^{L_{\text{cut}}}\left(\sigma_L^{(R\text{-matrix})} - \sigma_L^{(\text{FBA})}\right). \quad (8)$$

This means that the few lowest $\sigma_L^{(\text{FBA})}$ ($L < L_{\text{cut}}$) of the total cross sections within the FBA are replaced by the corresponding $\sigma_L^{(R\text{-matrix})}$. Beyond L_{cut} the difference between $\sigma_L^{(R\text{-matrix})}$ and $\sigma_L^{(\text{FBA})}$ is negligible. For the optical dipole-allowed transitions although the required numbers of PWCSs are much more than those of the monopole transitions, the L_{cut} values for these two different kinds of transitions are very close.

The R-matrix method is appropriate in low energy region, when the energy is higher to reach the intermediate energy region, the number of computational channels needed to be taken into account in the R-matrix calculation will increase rapidly, making the computational efforts also increase rapidly. In order to avoid the large computational efforts of the R-matrix calculation in the intermediate energy region, we perform distorted wave calculation in this corresponding region. The partial wave cross section within DW calculation is expressed in the similar form as Eq. (6), where the continuum wavefunction ϕ of the $N+1$ electron here is a distorted wave instead of the regular spherical Bessel functions in FBA PWCS. The distorted potential is the He ground state $1s^2$ potential. In the present DW calculation, we orthogonalize the continuum wavefunction to the target state wavefunctions, and take into account the exchange interactions as well as the direct ones. In this way, we are able to apply the DW approximation to neutral systems, such as e + He impact excitations. Here we also only need to replace the first few relevant $\sigma_L^{(\text{FBA})}$ with $\sigma_L^{(\text{DW})}$ to obtain the accurate total cross sections in the intermediate energy region, i.e.,

$$\sigma_{\text{total}}^{(\text{accurate})} = \sigma_{\text{total}}^{(\text{FBA})} + \sum_{L=0}^{L_{\text{cut}}}\sigma_L^{(\text{C})}$$
$$= \sigma_{\text{total}}^{(\text{FBA})} + \sum_{L=0}^{L_{\text{cut}}}\left(\sigma_L^{(\text{DW})} - \sigma_L^{(\text{FBA})}\right). \quad (9)$$

3. Computational results

In the present work, we calculate the e + He excitation cross sections for the spin-allowed transitions $1\,^1\text{S}$–$n\,^1\text{S}$ (n = 2–4) and $1\,^1\text{S}$–$n\,^1\text{P}$ (n = 2–4) using the 3 different methods to obtain the accurate total cross sections in the whole energy. The orbital bases 'Set 3' in our previous work[14] (i.e., n = 1–4 are spectroscopy orbitals and n = 5, 6 are pseudo orbitals) are adopted in the present calculations of the three methods, where adequate convergence of the target states can be achieved. We first perform total FBA calculations, i.e., Eq. (5), and partial wave FBA calculations, i.e., Eq. (6), in the whole energy region to readily obtain the total cross sections $\sigma_{\text{total}}^{(\text{FBA})}$ and FBA PWCS $\sigma_L^{(\text{FBA})}$. Then we perform the exact R-matrix calculations, i.e., Eq. (2), in the low energy region and

DW calculations, i.e., Eq. (9), in the intermediate energy region to obtain the corresponding $\sigma_L^{(R\text{-matrix})}$ and $\sigma_L^{(\mathrm{DW})}$. Finally by replacing the first few lowest $\sigma_L^{(\mathrm{FBA})}$ with the corresponding $\sigma_L^{(R\text{-matrix})}$ and $\sigma_L^{(\mathrm{DW})}$, i.e., Eqs. (8) and (9), we obtain the accurate total cross sections in the whole energy region based on the Born cross sections. The $\sigma_L^{(R\text{-matrix})}$ are calculated in the energy region of below 35 Ryd, and the $\sigma_L^{(\mathrm{DW})}$ are calculated in the energy region of 25–70 Ryd. Figure 1 shows the results of our calculations for the $1\,^1\mathrm{S}$–$n\,^1\mathrm{S}$ ($n = 2$, 3) and $1\,^1\mathrm{S}$–$n\,^1\mathrm{P}$ ($n = 2$, 3) transitions, compared with other calculation results and experimental measurements.[28–32] The blue lines are our calculated total Born cross sections, the black lines are accurate total R-matrix cross sections and the red lines are accurate total DW cross sections. For monopole transitions, the black lines merge to the red lines at about 30 Ryd, while for dipole transitions, these two lines merge earlier from about 25 Ryd. The red lines merge to the blue lines at about 40 Ryd, which means the FBA calculations are appropriate from here. Kim[40] has introduced a correction using three atomic parameters (i.e., the ionization energy, the excitation energy and the dipole oscillator strength value f) to improve the plane-wave Born cross sections for neutral atoms. His correction method is only applicable to spin- and electric dipole-allowed transitions with the accuracy of about 20%. The dashed dark grey lines are obtained by correcting the total Born cross sections (blue lines) using Kim's correction method. All the theoretical results are in agreement with the experimental data in the overall regions. However, our results show complex resonant structures in the low energy region near the thresholds, especially for the monopole transitions as shown in the inset of Fig. 1. More detailed resonant structures in the low energy region can be found in our previous work.[14]

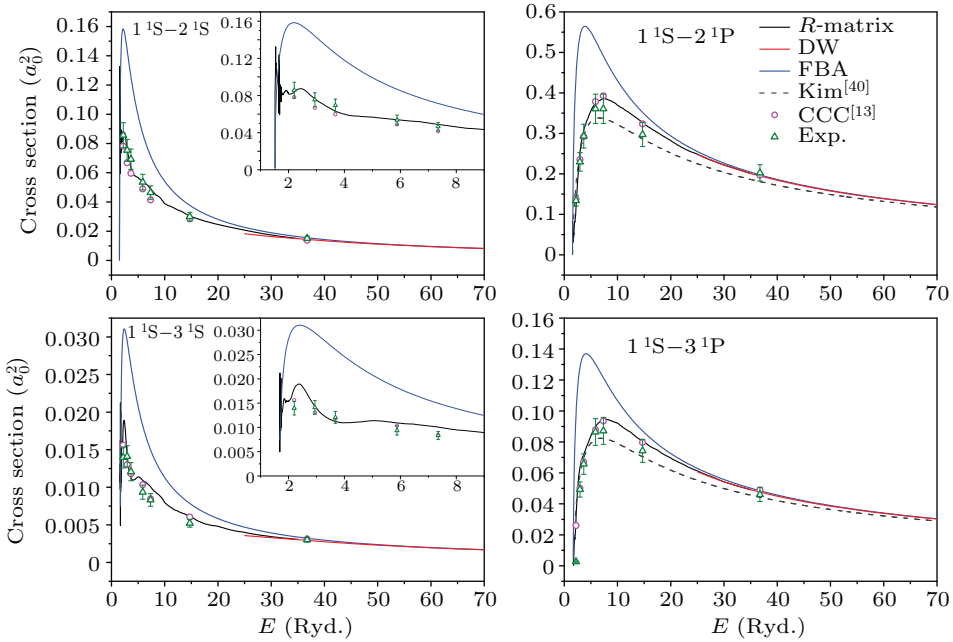


Fig. 1. Our calculated EIE cross sections for the $1\,^1\mathrm{S}$–$n\,^1\mathrm{S}$ ($n = 2$, 3) and $1\,^1\mathrm{S}$–$n\,^1\mathrm{P}$ ($n = 2$, 3) transitions, and the comparison with other calculations[13,40] and experimental measurements.[28–32]

Because the thresholds of different excitations are different, in order to compare our calculation results for different excitations on equal footing, we introduce the reduced incident energy, i.e., the incident energy over the excitation energy of the transition. Figure 2(a) shows the ratios of accurate total cross sections and total FBA cross sections of our calculations for $1\,^1\mathrm{S}$–$n\,^1\mathrm{S}$ ($n = 2$–4) transitions in reduced incident energies. The colored solid lines are ratios for R-matrix calculations, i.e., $\sigma_{\mathrm{total}}^{(R\text{-matrix})}/\sigma_{\mathrm{total}}^{(\mathrm{FBA})}$ and the colored dash lines are ratios for DW calculation, i.e., $\sigma_{\mathrm{total}}^{(\mathrm{DW})}/\sigma_{\mathrm{total}}^{(\mathrm{FBA})}$. Note that, there exist resonant structures in low reduced energy region because of the complex structures near the thresholds. The ratios for R-matrix calculation naturally interface with the corresponding ratios for DW calculation at around the reduced energy of about 20 for all the three $1\,^1\mathrm{S}$–$n\,^1\mathrm{S}$ ($n = 2$–4) transitions. The ratios for DW calculation gradually merge to 1 when the energy is high enough, which means the cross sections calculated by distorted wave method are equal to those by FBA. As the behavior and trend of the three ratios are similar and close to each other, we predict the ratios of all other higher transitions in this $1\,^1\mathrm{S}$–$n\,^1\mathrm{S}$ channel are also similar and close to the trend of these three ratios. Therefore we propose a universal correction function (CF) based on these three ratios, by which one can readily obtain the EIE cross section of any transitions in the same $1\,^1\mathrm{S}$–$n\,^1\mathrm{S}$ channel based on the readily calculated FBA cross sections. The CF labeled by $Y^{\mathrm{CF}}_{1\,^1\mathrm{S}-n\,^1\mathrm{S}}$ is a smooth curve with error bars in different regions as shown in Fig. 2(b). The errors come from the largest deviations between the CF

curve and three ratios. Therefore one can determine the accuracy of the cross sections obtained by the CF. The first error bar in the low energy region is very large because we use a smooth curve to represent the complex resonant structures here. The error bars became smaller as the energy increases.

We provide a data table for readers to use the correction function for the $1\,^1\mathrm{S}$–$n\,^1\mathrm{S}$ transitions ($Y^{\mathrm{CF}}_{1\,^1\mathrm{S}-n\,^1\mathrm{S}}$) as shown in Table 1 and a computer fortran subroutine in the supplementary materials in PDF format,[33] where the CF in any excitation energy $Y^{\mathrm{CF}}_{i-j}(E_\mathrm{i}/\Delta E_\mathrm{excit})$ could be readily obtained by interpolation. To facilitate different application requirements, we also propose an analytical formula

$$Y^{\mathrm{CF_Fit}}_{i-j}(x) = 1 - C_1\,\mathrm{e}^{-x/T_1} - C_2\,\mathrm{e}^{-x/T_2} - C_3\,\mathrm{e}^{-x/T_3}, \quad (x = E_\mathrm{i}/\Delta E_\mathrm{excit}). \tag{10}$$

The corresponding coefficients C_1, T_1, C_2, T_2, C_3, T_3 in the formula are shown in Table 3. With these coefficients, the CF curve is well reproduced as shown in Fig. 2(b).

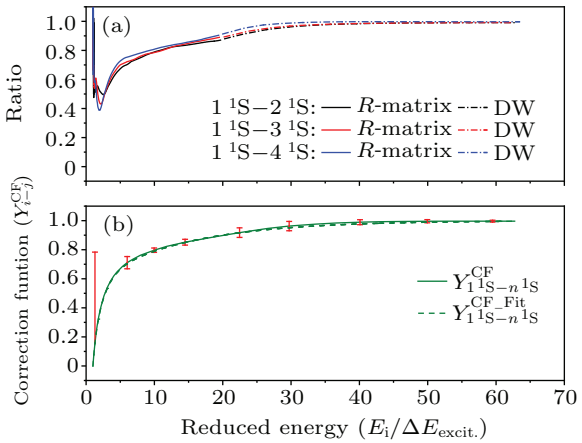


Fig. 2. (a) Ratios (accurate total cross sections over the total FBA cross sections) for $1\,^1\mathrm{S}$–$2\,^1\mathrm{S}$, $1\,^1\mathrm{S}$–$3\,^1\mathrm{S}$ and $1\,^1\mathrm{S}$–$4\,^1\mathrm{S}$ transitions. The colored solid lines are ratios for R-matrix calculations, i.e., $\sigma^{(R\text{-matrix})}_{\mathrm{total}}/\sigma^{(\mathrm{FBA})}_{\mathrm{total}}$. The colored dash lines are ratios for DW calculation, i.e., $\sigma^{(\mathrm{DW})}_{\mathrm{total}}/\sigma^{(\mathrm{FBA})}_{\mathrm{total}}$. (b) Correction functions for $[1s^2]\,1\,^1\mathrm{S}$–$[1sns]\,n\,^1\mathrm{S}$ transitions $Y^{\mathrm{CF}}_{1\,^1\mathrm{S}-n\,^1\mathrm{S}}$ and corresponding analytical curve $Y^{\mathrm{CF_Fit}}_{1\,^1\mathrm{S}-n\,^1\mathrm{S}}$. Correction function for $1\,^1\mathrm{S}$–$n\,^1\mathrm{S}$ is obtained by summarizing the ratios in (a). Reduced energy is the ratio between the incident energy E_i and the transition excitation energy E_excit.

Table 1. Correction function data for $[1s^2]\,1\,^1\mathrm{S}-[1sns]\,n\,^1\mathrm{S}$ transitions.

1	0	3	0.52797	6.5	0.72488	13	0.83586	26	0.94266	46	0.99447
1.2	0.11101	3.2	0.54984	7	0.73865	14	0.84664	28	0.95395	48	0.99534
1.4	0.19865	3.4	0.56825	7.5	0.75106	15	0.85628	30	0.96369	50	0.99612
1.6	0.26989	3.6	0.5859	8	0.76301	16	0.86485	32	0.97076	55	0.99622
1.8	0.32602	3.8	0.60099	8.5	0.77161	17	0.87343	34	0.97731	60	0.99632
2	0.37142	4	0.61608	9	0.78022	18	0.882	36	0.98226	65	0.99632
2.2	0.41284	4.5	0.64522	9.5	0.78882	19	0.8902	38	0.98609		
2.4	0.4465	5	0.66938	10	0.79729	20	0.89814	40	0.98934		
2.6	0.48017	5.5	0.69151	11	0.81158	22	0.91403	42	0.99163		
2.8	0.50461	6	0.7104	12	0.82509	24	0.92854	44	0.99337		

Table 2. Correction function data for $[1s^2]\,1\,^1\mathrm{S}-[1snp]\,n\,^1\mathrm{P}$ transitions.

1	0	3	0.62774	6.5	0.87707	13	0.96458	26	0.98678	46	0.99668
1.2	0.14639	3.2	0.6529	7	0.8916	14	0.96771	28	0.98853		
1.4	0.26397	3.4	0.67814	7.5	0.9041	15	0.97083	30	0.99005		
1.6	0.34364	3.6	0.7006	8	0.9147	16	0.97396	32	0.99139		
1.8	0.40207	3.8	0.72165	8.5	0.9237	17	0.97562	34	0.99243		
2	0.45436	4	0.74261	9	0.93153	18	0.97724	36	0.99337		
2.2	0.49998	4.5	0.78521	9.5	0.93799	19	0.97887	38	0.99417		
2.4	0.54036	5	0.81508	10	0.94376	20	0.98027	40	0.99486		
2.6	0.57367	5.5	0.84018	11	0.95336	22	0.98295	42	0.9955		
2.8	0.60166	6	0.86165	12	0.96023	24	0.98496	44	0.99609		

Table 3. The coefficients of the analytical formulas $Y^{\mathrm{CF_Fit}}_{i-j}$ for the correction functions Y^{CF}_{i-j} ($a(b)$ represent $a\times 10^b$).

$i-j$	$1\,^1\mathrm{S}$–$n\,^1\mathrm{S}$	$1\,^1\mathrm{S}$–$n\,^1\mathrm{P}$
C_1	4.39(−1)	5.37(0)
T_1	1.35(1)	3.05(−1)
C_2	9.44(−1)	1.12(0)
T_2	1.48(0)	2.30(0)
C_3	1.47(0)	8.00(−2)
T_3	3.89(−1)	1.39(1)

Figure 3(a) shows the ratios of accurate total cross sections and total FBA cross sections of our calculations for $1\,^1\mathrm{S}$–$n\,^1\mathrm{P}$ (n = 2–4) transitions in reduced incident energies. The ratios for R-matrix calculation naturally interface with the corresponding ratios for DW calculation at around the reduced energy about 15 for all the 3 $1\,^1\mathrm{S}$–$n\,^1\mathrm{P}$ (n = 2–4) transitions. Similar to the $1\,^1\mathrm{S}$–$n\,^1\mathrm{S}$ transitions, there exist resonant structures in the low reduced energy region. While in the high energy region, the ratios for DW calculation gradually merge to 1, which means the cross sections calculated by distorted wave method are equal to those by FBA. The ratios of Kim's scaled cross sections[40] are also displayed. Compared to our ratios,

Kim's ratios merge to 1 more slowly. Based on the similar behavior and trend of the 3 ratios, we also propose a universal correction function for the $1\,^1\mathrm{S}$–$n\,^1\mathrm{P}$ transitions ($Y^{\mathrm{CF}}_{1\,^1\mathrm{S}-n\,^1\mathrm{P}}$) by which one can easily obtain the cross section of any transitions in the same $1\,^1\mathrm{S}$–$n\,^1\mathrm{P}$ channel based on the readily calculated FBA cross sections. As shown in Fig. 3(b), the error bars of the CF in $1\,^1\mathrm{S}$–$n\,^1\mathrm{P}$ transition channel $Y^{\mathrm{CF}}_{1\,^1\mathrm{S}-n\,^1\mathrm{P}}$ are smaller than those of the CF in $1\,^1\mathrm{S}$–$n\,^1\mathrm{S}$ channel $Y^{\mathrm{CF}}_{1\,^1\mathrm{S}-n\,^1\mathrm{S}}$ due to the larger cross sections of the electric dipole-allowed transitions. Interesting to note that, the $Y^{\mathrm{CF}}_{1\,^1\mathrm{S}-n\,^1\mathrm{P}}$ merges to 1 more rapidly than $Y^{\mathrm{CF}}_{1\,^1\mathrm{S}-n\,^1\mathrm{S}}$. This is because for the optical dipole-allowed transition, a large number of PWCSs are needed to be taken into account, the L_{cut} in Eq. (8) is relatively smaller than that of $1\,^1\mathrm{S}$–$n\,^1\mathrm{S}$ transitions. The detailed $Y^{\mathrm{CF}}_{1\,^1\mathrm{S}-n\,^1\mathrm{P}}$ is shown in Table 2. A computer fortran subroutine is also provided in the supplementary materials in PDF format,[16] as well as the coefficients of Eq. (10) in Table 3 with the resultant curve $Y^{\mathrm{CF_Fit}}_{1\,^1\mathrm{S}-n\,^1\mathrm{P}}$ shown in the Fig. 3(b).

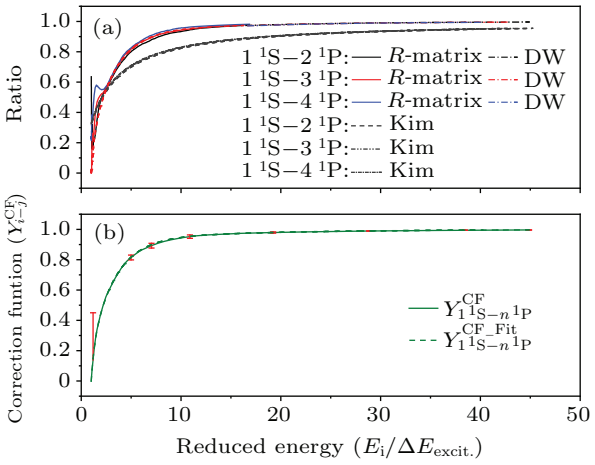


Fig. 3. (a) Ratios (accurate total cross sections over the total FBA cross sections) for $1\,^1\mathrm{S}$–$2\,^1\mathrm{P}$, $1\,^1\mathrm{S}$–$3\,^1\mathrm{P}$ and $1\,^1\mathrm{S}$–$4\,^1\mathrm{P}$ transitions. The colored solid lines are ratios for R-matrix calculations, i.e., $\sigma^{(R\text{-matrix})}_{\mathrm{total}}/\sigma^{(\mathrm{FBA})}_{\mathrm{total}}$. The colored dash lines are ratios for DW calculation, i.e., $\sigma^{(\mathrm{DW})}_{\mathrm{total}}/\sigma^{(\mathrm{FBA})}_{\mathrm{total}}$. (b) Correction functions for $[1s^2]\ 1\,^1\mathrm{S}$–$[1snp]$–$n\,^1\mathrm{P}$ transitions $Y^{\mathrm{CF}}_{1\,^1\mathrm{S}-n\,^1\mathrm{P}}$ and corresponding analytical curve $Y^{\mathrm{CF_Fit}}_{1\,^1\mathrm{S}-n\,^1\mathrm{P}}$. Correction function for $1\,^1\mathrm{S}$–$n\,^1\mathrm{P}$ is obtained by summarizing the ratios in (a). Reduced energy is the ratio between incident energy E_{i} and the transition excitation energy E_{excit}.

4. Discussion and conclusion

Finally, we would like to conclude with the following remarks. With our proposed effective method to calculate the EIE cross sections with enough accuracy in the whole energy region by combination of R-matrix method, DW method and FBA methods in the low, intermediate and high energy regions respectively, accurate e + He collisional excitation cross sections from the ground state to the final $n\,^1\mathrm{S}$ ($n = 2$–4) and $n\,^1\mathrm{P}$ ($n = 2$–4) states are calculated, which are in good agreement with the available experiments.[28–32] By studying the ratios (accurate total cross sections over Born cross sections) within the same channel, we find that these ratios have similar behaviors and are close to each other, which means they have the same channel properties. Although the calculated ratios in Figs. 2(a) and 3(a) do not show strict convergent behavior, it is interesting to note that the channel property of these ratios in the high energy region is understandable from the analysis of the related cross sections. More specifically, the ratio in the high energy region could be calculated as the ratio between the DW cross section and FBA cross section. As shown in Ref. [44] for the DW electron impact excitation cross sections and Eq. (5) for those FBA cross sections, both cross sections can be factorized as a one-body matrix element defined only on the involved target states and a smooth function of the excitation energy. The channel property of the first part stems from the channel property of the excited target wavefunctions,[45,46] whereas that of the second part stems from the fact that the change in the excitation energy would be smaller and smaller when the excitation degree increases (the excitation energy would ultimately converge to the ionization energy). Based on this argument, we expect the channel property in our defined ratio would be a universal one in general atomic systems. Therefore we propose a universal correction function (CF) Y^{CF}_{i-j} based on these properties for the calculation of all highly excited final states in the same channel. By utilizing the correction function, one can conveniently obtain the EIE cross sections of any transition in the same excitation channel in the whole energy region based on the Born cross sections. The CF is a smooth curve with error bars in different energy regions, which should be convenient for one to estimate the accuracy of the calculated cross sections. In our case, the largest error bars are in the low energy region due to various resonant structures. For applications sensitive to the precisions of EIE cross sections in that region, a direct usage of the R-matrix calculation results is preferred. The CF for He EIE cross sections from the ground state to the final $n\,^1\mathrm{S}$ and $-n\,^1\mathrm{P}$ states with arbitrary n are provided as shown in Tables 1 and 2 (also Ref. [33] for a fortran subroutine in the supplementary materials in PDF format), as well as the fitting formula Eq. (10) with the corresponding coefficients shown in Table 3. In this way, the accurate EIE cross section can be acquired by the formula $\sigma^{\mathrm{accurate}}_{\mathrm{total}}(E_{\mathrm{i}}) = Y^{\mathrm{CF}}_{i-j}(E_{\mathrm{i}}/\Delta E_{\mathrm{excit}}) \cdot \sigma^{\mathrm{FBA}}_{\mathrm{total}}(E_{\mathrm{i}})$ for the transitions $i - j$ ($1\,^1\mathrm{S}$–$n\,^1\mathrm{S}$ and $1\,^1\mathrm{S}$–$n\,^1\mathrm{P}$).

Note that although some empirical quasi-universal scaling factors to correct the first Born cross sections have been proposed,[40,47–50] they are not applicable in general cases and with limited accuracies. For instance, Tian and Li[48] proposed a correction function by which one can obtain the spin-allowed EIE cross sections from FBA cross sections with an accuracy of about 50%. Kim introduced a correction using three atomic properties (i.e., the ionization energy, the excitation energy and the dipole f value) to improve the plane-wave Born cross

sections for electron-impact excitation of neutral atoms[40] and singly charged ions[50] for spin and electric dipole-allowed transitions with an accuracy of about 20%. On the other hand, the universal correction functions we proposed can not only apply to spin-allowed transitions, which have been shown in the present work, but also to the spin-forbidden transitions. Because they are obtained from the ratios of the calculated accurate cross sections and the readily obtained approximated cross sections, which should be very flexible. In addition to neutral atoms, our proposed correction functions should be also valid for various degrees of ionized atoms by considering the Elwert factor at the thresholds.[51] Furthermore, the calculations from the ground state to the final channels in the present work can be extended to the case of any excited states to final channels,[18] and even for the case of any initial channels to any final channels,[52] which could be very useful in providing precise total cross sections in the whole energy region for many research fields, such as astrophysics studies and inertial confinement fusion research.

Data availability statement

The data that support the findings of this study are openly available in Science Data Bank at https://doi.org/10.57760/sciencedb.j00113.00142.

Acknowledgment

Project supported by the National Natural Science Foundation of China (Grant No. 12241410).

References

[1] Peimbert A, Peimbert M and Luridiana V 2002 *Astrophys. J.* **565** 668
[2] Luridiana V, Peimbert A, Peimbert M and Cervino M 2003 *Astrophys. J.* **592** 846
[3] Peimbert M, Luridiana V and Peimbert A 2007 *Astrophys. J.* **666** 636
[4] Clegg R E S 1987 *Mon. Not. R. Astron. Soc.* **229** 31
[5] Kingdon J and Ferland G J 1995 *Astrophys. J.* **442** 714
[6] Bederson B and Kieffer L J 1971 *Rev. Mod. Phys.* **43** 601
[7] Heddle D W O and Gallagher J W 1989 *Rev. Mod. Phys.* **61** 221
[8] Nakazaki S 1993 *Adv. At. Mol. Opt. Phy.* **30** 1
[9] Berrington K A, Burke P G, Freitas L C G and Kingston A E 1985 *J. Phys. B: At. Mol. Phys.* **18** 4135
[10] Sawey P and Berrington K 1993 *At. Data Nucl. Data Tables* **55** 81
[11] Bartschat K 1998 *J. Phys. B: At. Mol. Opt. Phys.* **31** L469
[12] Stepanović M, Minić M, Cvejanović D, Jureta J, Kurepa J, Cvejanović S, Zatsarinny O and Bartschat K 2006 *J. Phys. B: At. Mol. Opt. Phys.* **39** 1547
[13] Fursa D V and Bray I 1995 *Phys. Rev. A* **52** 1279
[14] Zeng D L, Gao X, Han X Y and Li J M 2015 *Phys. Rev. A* **91** 022707
[15] Chang J J 1977 *J. Phys. B: At. Mol. Phys.* **10** 3335
[16] Norrington P H and Grant I P 1987 *J. Phys. B: At. Mol. Phys.* **20** 4869
[17] Ait-Tahar S, Grant I P and Norrington P H 1996 *Phys. Rev. A* **54** 3984
[18] Gao X, Jin R, Zeng D L, Han X Y, Yan J and Li J M 2015 *Phys. Rev. A* **92** 052712
[19] Han X Y, Li Y M, Zhang H, Yan J, Li J M and Voky L 2008 *Phys. Rev. A* **78** 052702
[20] Han X Y and Li J M 2006 *Phys. Rev. A* **74** 062711
[21] Han X Y, Zeng D L, Gao X and Li J M 2015 *Chin. Phys. B* **24** 083103
[22] Inokuti M 1971 *Rev. Mod. Phys.* **43** 297
[23] Oppenheimer J R 1928 *Phys. Rev.* **32** 361
[24] Ochkur V I 1964 *Sov. Phys. JETP* **18** 503
[25] Inokuti M 1967 *J. Phys. Soc. Japan* **22** 971
[26] Joachain J C and Roper L D 1976 *Phys. Today* **29** 53
[27] Drake G W F 2006 *Springer Handbook of Atomic, Molecular, and Optical Physics* (Windsor: Springer) p. 716
[28] Register D F, Trajmar S and Srivastava S K 1980 *Phys. Rev. A* **21** 1134
[29] Montague R G, Harrison M F A and Smith A C H 1984 *J. Phys. B: At. Mol. Phys.* **17** 3295
[30] Nickel J C, Imre K, Register D F and Trajmar S 1985 *J. Phys. B: At. Mol. Phys.* **18** 125
[31] Kauppila W E, Stein T S, Smart J H, Dababneh M S, Ho Y K, Downing J P and Pol V 1981 *Phys. Rev. A* **24** 725
[32] de Heer F J, Hoekstra R, Kingston A E and Summers H P 1992 *Nucl. Fusion Suppl.* **3** 19
[33] Sun R, Zeng D L, Jin R, Han X Y, Gao X and Li J M 2022 *See supplemental materials for a fortran subroutine providing the CF of helium atom*
[34] Berrington K A, Eissner W B and Norrington P H 1995 *Comput. Phys. Commun.* **92** 290
[35] Bethe H 1930 *Ann. Phys.* **397** 325
[36] Tian B G and Li J M 1984 *Acta Phys. Sin.* **33** 1401 (in Chinese)
[37] Pan X C and Li J M 1985 *Acta Phys. Sin.* **34** 1500 (in Chinese)
[38] Han X Y, Lan V and Li J M 2004 *Chin. Phys. Lett.* **21** 54
[39] Liang X L, Pan X C, Li J M and Lee C M 1985 *Chin. Phys. Lett.* **2** 545
[40] Kim Y K 2001 *Phys. Rev. A* **64** 032713
[41] Coz M 1973 *Nucl. Technol.* **18** 313
[42] Joachain J C and Roper L D 1976 *Phys. Today* **29** 53
[43] McCarthy I E and Weigold E 1995 *Electron-Atom Collisions* (Cambridge: Cambridge University Press) pp. 196–198
[44] Bar Shalom A, Klapisch M and Oreg J 1988 *Phys. Rev. A* **38** 1773
[45] Seaton M J 1983 *Rep. Prog. Phys.* **46** 167
[46] Gao X, Han X Y and Li J M 2016 *J. Phys. B: At. Mol. Opt. Phys.* **49** 214005
[47] Li J M 1980 *Acta. Phys. Sin.* **29** 419 (in Chinese)
[48] Tian B G and Li J M 1986 *Acta. Phys. Sin.* **35** 203 (in Chinese)
[49] Qu Y Z, Wang J G, Tong X M and Li J M 1995 *Chin. Phys. Lett.* **12** 581
[50] Kim Y K 2002 *Phys. Rev. A* **65** 022705
[51] Elwert G and Haug E 1969 *Phys. Rev.* **183** 90
[52] Zhu C, Wang J G, Qu Y Z and Li J M 1998 *Phys. Rev. A* **57** 1747